



computational proteomics

## Laboratory for Computational Proteomics

[www.FenyoLab.org](http://www.FenyoLab.org)

E-mail: [Info@FenyoLab.org](mailto:Info@FenyoLab.org)

Facebook: [NYUMC Computational Proteomics Laboratory](#)

Twitter: [@CompProteomics](#)

## Molecular-dynamics study of electronic sputtering of large organic molecules

D. Fenyő, B. U. R. Sundqvist, and B. R. Karlsson

*Department of Radiation Sciences, Uppsala University, Box 535, S-751 21 Uppsala, Sweden*

R. E. Johnson

*Department of Nuclear Engineering and Engineering Physics, University of Virginia, Charlottesville, Virginia 22901*

(Received 26 June 1989; revised manuscript received 29 December 1989)

In order to describe electronic sputtering of large organic molecules from a solid as a result of the passage of a fast heavy ion, a molecular-dynamics calculation was carried out. A modified Lennard-Jones potential is used to describe the intermolecular interaction. When the ion passes through the organic solid, the excited molecules near the ion track are assumed to expand due to the energy deposited so that the forces between them become repulsive. Both excited and unexcited molecules are ejected due to the compression wave emitted from the track. Sputtering yields as well as angular and velocity distributions of ejected molecules were studied as functions of energy input, angle of incidence, and material cohesive energy. The results are consistent with a number of experimental observations and our analytical model.

### INTRODUCTION

In 1974, Macfarlane and co-workers<sup>1</sup> showed that small thermally labile organic molecules could be ejected into the gas phase by irradiating a solid sample with fission fragments. Today, large organic molecules (up to 45 000 u) can be transferred to the gas phase by irradiation with fast heavy ions ( $\sim 1$  MeV/u).<sup>2</sup> This ejection of the molecules is called electronic sputtering because fast ions lose their energy primarily in collisions with target electrons, and in insulators these electronic excitations remain localized long enough for conversion into atomic motion which can lead to ejection. Whereas the desorption of atoms and atomic ions<sup>3</sup> or the sputtering of small molecules from low-temperature condensed gas solids<sup>4</sup> can occur in response to individual excitations, the ejection of large species requires a number of closely spaced excitation events.<sup>5,6</sup> Fast heavy ions are ideal in this regard as they produce a cylindrical region of high-excitation density (a track). Several mechanisms have been described to explain how the electronic energy is transferred into atomic motion in this region: Coulomb repulsion<sup>7</sup> between ionized atoms, repulsive decay of excited and ionized molecules,<sup>8</sup> and molecular expansion due to vibrational excitation produced by the secondary electrons<sup>9</sup> and during electronic recombination.<sup>6</sup> These processes all lead to a local expansion of the solid.<sup>6</sup> In addition, a number of models have been proposed in order to describe the ejection in response to this excited track. These can be divided into two classes:<sup>10</sup> those in which the probability of ejection is determined by the energy density at the surface<sup>11-12</sup> (activated surface or "thermal" spike models) and those in which a volume of material is ejected in response to the momentum of expansion at the surface.<sup>13-15</sup> Whereas the former ejection process has been shown to describe the electronic sputtering of low-temperature condensed-gas solids, it is becoming clear now that the latter process is more consistent

with aspects of electronic sputtering of large organic molecules. Here we present molecular-dynamics calculations for the ejection of large molecules in which the result of the excitation by the incident ion is the production of expanded molecules.

Models for the ejection of large molecules have typically been compared to secondary ion yields as a function of the stopping power, velocity, charge state, or angle of incidence.<sup>16-18</sup> These comparisons have been hampered by uncertainties in the ion versus neutral production probabilities. However, recent data on total yields of neutral whole molecules<sup>19,20</sup> and on axial<sup>21</sup> and radial<sup>22</sup> velocity distributions of the whole ions ejected allow us to make critical tests on the aspects of the ejection process.<sup>10,14,23</sup> These data are compared here to results from a molecular-dynamics description of the behavior of the molecules in the excited track.

The molecular-dynamics (MD) technique is suitable for calculating properties of systems consisting of a large number of classical particles. Newton's law of motion for the system is approximated using a difference equation which gives the motion of each particle as a function of time. MD was introduced in 1957 by Alder and Wainwright.<sup>24</sup> Since then, MD has been applied to many different problems where analytical solutions are not possible and simple models are not very helpful, e.g., time-dependent properties of liquids,<sup>25</sup> protein structure,<sup>26</sup> radiation damage,<sup>27</sup> nuclear sputtering,<sup>28</sup> and laser-induced ablation of organic solids.<sup>29</sup> The MD technique is used here to investigate the sputtering of large organic molecules under the assumption that the incident ion produces a track of expanded molecules. Preliminary results from this calculation were presented earlier<sup>14</sup> and inspired the development of a related analytical approximation for the ejection process<sup>10</sup> which is tested here.

### THE MODEL

In the calculations presented here we do not investigate the cause of the expansion of the molecules in the

track. Rather, we assume that in response to the excitations the molecules in a cylindrical region around the track expand radially of the order of 10% (Ref. 9) due to one or more of the effects discussed above. In order to describe in a simple but quantitative way the result of this expansion molecules were assumed to be spherical and the forces between them were described by a Lennard-Jones potential:

$$V(d) = E_b [(d_0/d)^{12} - 2(d_0/d)^6], \quad (1)$$

where  $E_b$  is a binding energy. The parameters  $E_b$  and  $d_0$  were chosen to give the solid sample a reasonable cohesive energy and density. In addition, to obtain a reasonable value for the velocity of sound in the medium a hard core ( $r_c$ ) was introduced (Fig. 1). Therefore,  $d$  in the expression for the potential was chosen to be the closest distance between these hard cores:

$$d = |\mathbf{x}_i - \mathbf{x}_j| - 2r_c. \quad (2)$$

The distance ( $d_0$ ) between the cores that gives the minimum potential energy for two neighbors is

$$d_0 = r_i + r_j - 2r_c = 2(r_0 - r_c) + \Delta r_i + \Delta r_j, \quad (3)$$

where  $r_i, r_j$  are the radii,  $\Delta r_i, \Delta r_j$  are the radial expansions of the two molecules, and  $r_0$  is the molecular radius calculated from the density. The core radius ( $r_c$ ) was chosen to give a Young's modulus of  $\sim 10^{10}$  N/m<sup>2</sup>.<sup>9</sup> This gave  $2.6 \times 10^3$  and  $2.1 \times 10^3$  m/s for the longitudinal and transverse elastic wave velocities, respectively, for the sample used in the simulations. These velocities were measured by introducing a small perturbation at one end of the lattice and simulating its propagation. When an excited molecule expands, the radius of the molecule ( $r$ ) is altered from  $r_0$  to  $r_0 + \Delta r$ . The potential will become repulsive as shown in Fig. 2 and the change in potential energy introduced is given by substituting Eq. (3) into Eq. (1). Such repulsive forces between neighbors in the track region will result in a net expansion of the solid. If very few molecules are excited or the level of excitation is low, ejection will not occur. However, exciting a sufficient number of molecules will guarantee ejection<sup>10,14,23</sup> These simulations have some similarities with those of Garrison and Srinivasan<sup>29</sup> who performed a calculation of ablation due to laser excitation of an organic solid. In their work, expanded molecules also interacted through a repulsive force. However, they did not have any residual attractive

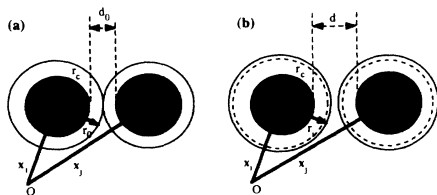


FIG. 1. (a) Two molecules at the potential energy minimum are shown prior to expansion. (b) Two molecules are shown after the expansion.

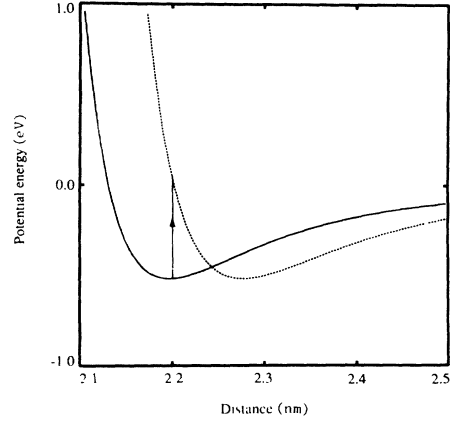


FIG. 2. The potential between two nonexpanded molecules (solid line) and the potential between two expanded molecules (dashed line).

force and, therefore, all excited molecules were driven off. In our calculations the effect of the expansion was limited by the cohesive forces of the material which is a more realistic picture. Recently Cui and Johnson<sup>23</sup> calculated sputtering yields in response to a track of vibrationally excited, light diatomic molecules and Lee and Lucchese<sup>30</sup> did a similar calculation for a linear array of excited molecules. The vibrational excitation results in a net expansion and both studies showed that the internal energy is rapidly converted into center of mass motion as originally proposed in the Williams and Sundqvist model.<sup>9</sup> Therefore, we ignore the internal structure here, allowing us to make more extensive calculations and comparisons with the available data and then testing important parameters in the ejection process.

In this paper, we investigate sputtering caused by fast ions in charge-state equilibrium having a penetration distance much longer than the sample thickness. This makes the energy deposition constant along the ion track. The case of sputtering by slow ions losing their energy mainly in collision cascades could be treated similarly although the geometry of the energy deposition along the ion trajectory can differ.

## THE SIMULATIONS

The Verlet algorithm<sup>24</sup> was used to calculate the trajectories of the molecules

$$\mathbf{x}_i^{n+1} = 2\mathbf{x}_i^n - \mathbf{x}_i^{n-1} + \frac{\Delta t^2}{m_i} \mathbf{F}_i^n, \quad (4)$$

where  $\mathbf{x}_i^n$  is the position of molecule  $i$  at time  $n \Delta t$  and  $\mathbf{F}_i^n$  is the force on that molecule. A cylindrical sample with 1953 molecules in seven layers, each molecule having a mass of  $10^4$  u and a radius of 11 Å, was used for the simulations. The sample was adsorbed to an infinitely heavy plane substrate. The molecule-substrate potential was assumed to be the same as the intermolecular potential. In order to avoid focusing of impulses along lattice directions an unordered sample was used. This was created by building up circles of molecules with their center of mass

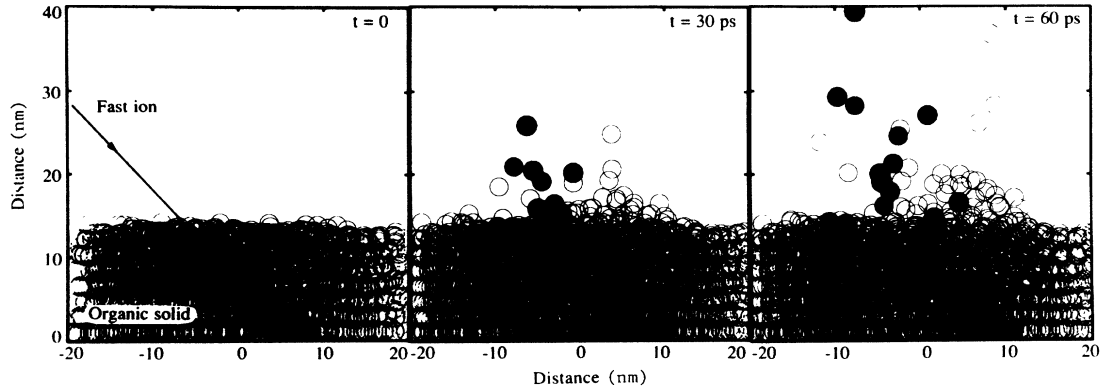


FIG. 3. The sample 0, 30, and 60 ps after the expansion of the molecules in the ion track. Expanded and nonexpanded molecules are shown as solid and open circles, respectively.

at  $R=2nr_0$ ,  $n=0, \dots, N$  ( $R$  is the distance from the cylinder axis). In each of these circles, the molecules were placed in close-packed positions. The azimuthal angle, around the cylinder axis, for the first molecule in each circle was chosen randomly. The total number of molecules in the sample is given by

$$k \left[ 1 + \sum_{n=1}^N \left[ \frac{\pi}{\arcsin(1/2n)} \right] \right], \quad (5)$$

where  $k$  is the number of layers,  $N$  the number of circles, and  $[x]$  is defined as the largest integer less or equal to  $x$ . These molecules were not at the potential energy minimum and, therefore, prior to the simulation of the fast heavy-ion impact, the system was cooled to room temperature by taking away 0.01% of the resulting kinetic energy in each time step and then let it reach thermal equilibrium. The thickness of the sample did not change significantly during the cooling procedure. The sum of the binding energy of a molecule to the other molecules in this unordered sample is a broad distribution. The cohesive energy is taken to be the centroid of this distribution. At time zero, the molecules in a cylinder around the ion track were expanded and the propagation of the motion was simulated using a time step of  $10^{-14}$  s (Fig. 3). This time step gave fluctuations in the total energy of less than 1% of the expansion energy. Shorter time steps gave better energy conservation, however, the trajectories did not change significantly. The expansion was chosen to be homogeneous inside a chosen cylindrical region and

zero outside. For molecules partly inside the cylinder, the expansion was averaged over the volume. Cohesive energy, expansion, angle of incidence, and sample thickness were varied and the effects on erosion yield and on angular and velocity distributions of ejected molecules were studied. The statistics are sometimes poor since even for the simple nature of the excitation described the simulation of the effect of one incident ion for  $2 \times 10^{-10}$  s took about 48 h on a VAX station 2000. The finite size of the sample introduces artificial boundaries which could also affect the results. In this study, free boundaries have been used on all sides for the substrate which was reflecting. The effect of the finite radial size of the sample was tested by changing the diameter of the sample using 3962 molecules. The difference in yield between the two samples was within the variations due to sample inhomogeneity.

## RESULTS

When the compression wave from the expanding track reaches the surface, molecules are ejected. The molecules remaining in the solid eventually find new equilibrium positions and, typically, a crater is formed at the point of impact. This crater has a volume somewhat greater than the total volume of the ejected molecules due to pile up at the edges. In addition, for normal incidence the radial extent and depth are roughly equal (Fig. 4). This is the result found in our analytical model<sup>10</sup> but very different from that predicted by spike models,<sup>6</sup> and therefore the

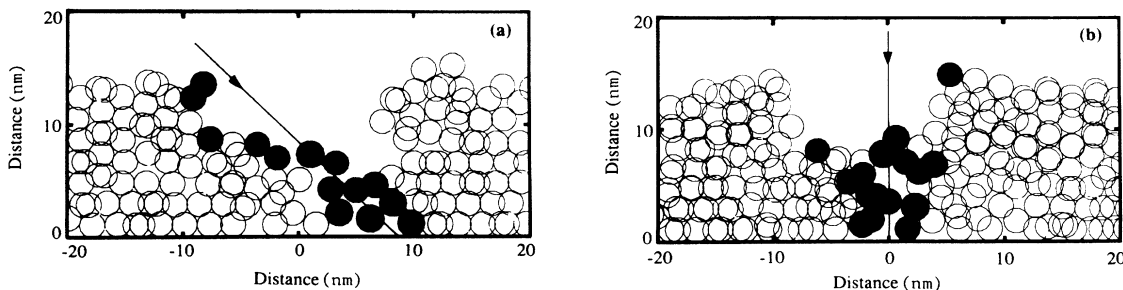


FIG. 4. Two examples of a cross section of the sample in the plane of incidence at  $2.10^{10}$  s after expansion for (a)  $45^\circ$  and (b)  $0^\circ$  angle of incidence. This shows the craters created in the sputtering process.

crater shape is indicative of the impulsive nature of the ejection process. In the following we discuss the behavior of the ejected molecules. The interpretation of the results is based on the following assumption: the nonexpanded molecules correspond to intact molecules in real experiments and the expanded molecules correspond to molecules which are likely to fragment.

### Sputtering yield

The yield ( $Y$ ) of the ejected nonexpanded molecules was studied as a function of the energy deposition per unit path length  $[(dE/dx)_{\text{eff}}]$ , i.e., the difference in potential energy before and immediately after expansion divided by the ion path length. Figures 5(a) and 5(b) show the yield at  $0^\circ$  and  $45^\circ$  angle of incidence, respectively. The track radius was  $19 \text{ \AA}$  and the sample thickness  $144 \text{ \AA}$ . Within the uncertainties due to sample inhomogeneity,  $Y$  varies as the third power of the energy deposition for normal incidence. The solid line in Fig. 5(a) is a least-squares fit to the data resulting in a power of  $2.8 \pm 0.2$ . For  $45^\circ$  angle of incidence, the yield varies roughly as the energy deposition to the third power in the lower part of the energy deposition region studied. Assuming  $(dE/dx)_{\text{eff}}$  to be proportional to the energy deposited per unit path length of the incident ion, i.e., the stopping power  $(dE/dx)$ , this dependence is consistent with measurements of whole molecule ejection yields<sup>20</sup> and with our preliminary calculations.<sup>14</sup> Including the ejected expanded molecules the dependence stays cubic for high-excitation densities which is consistent with the dependence found at high-excitation density for a track of vibrationally excited light diatoms<sup>23</sup> and with our analytical model.<sup>10</sup>

At the higher values of  $(dE/dx)_{\text{eff}}$ , the yield in Fig. 5(b) is seen to increase slower than  $[(dE/dx)_{\text{eff}}]^3$  for  $45^\circ$

angle of incidence. This is due to the limited thickness of the sample and represents the case of a thin layer being desorbed by a heavy ion. Normal incidence should give a similar change in dependence at higher-excitation densities. However, this was not studied because of the limited radial size of the sample. Two different sample thicknesses were investigated for low-excitation densities in the track. Although the yield decreased in magnitude for the smaller thickness, it varied as the third power of the energy deposition per unit path length for both thickness. The dependence of the yield on the cohesive energy [Fig. 5(b)] was also investigated. The yield was found to be independent of the cohesive energy ( $U$ ) when plotted as a function of  $(dE/dx)_{\text{eff}}/U$  also consistent with the analytical model.<sup>10</sup> Finally, the yield increases with angle of incidence faster than that found for a cylindrical thermal spike process.<sup>31</sup>

To determine whether or not a molecule was desorbed, its distance from the sample surface was used as a criterion. Varying the critical distance does not affect the scaling with excitation energy. However, the absolute yield changes as indicated by the error bars in Figs. 5(a) and 5(b), when varying the critical distance to the surface from  $d$  to  $d + 3r_0$ , where  $d$  is the sample thickness and  $r_0$  is the molecular radius. The total simulation time was made large enough ( $2 \times 10^{-10} \text{ s}$ ) and the yield does not change significantly for longer times. The first molecules leave the sample in  $\sim 10^{-11} \text{ s}$ ; at  $\sim 10^{-10} \text{ s}$ , the yield saturates.

### Angular and velocity distributions

In Figs. 6 and 7, the angular and the radial and axial velocity distributions of ejected molecules are shown for  $45^\circ$  and  $0^\circ$  angle of incidence, respectively. The definitions of radial and axial velocity are given in the

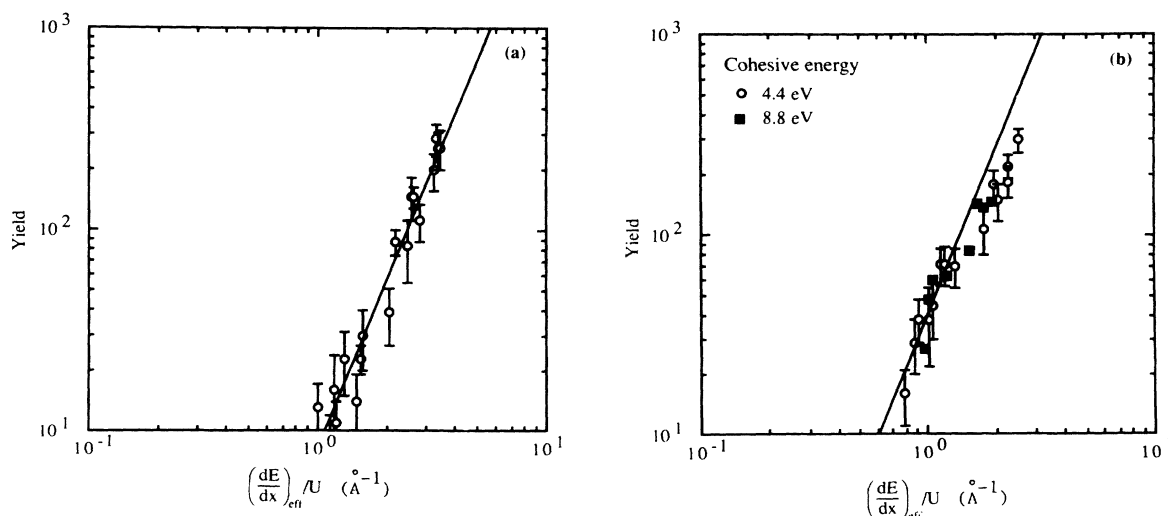


FIG. 5. Sputtering yield of nonexpanded molecules as a function of the effective stopping power  $(dE/dx)_{\text{eff}}$  divided by the cohesive energy ( $U$ ) for (a) normal incidence— a sample thickness ( $d$ ) of  $144 \text{ \AA}$  and  $U=4.4 \text{ eV}$ ; and (b)  $45^\circ$  angle of incidence—  $d=144 \text{ \AA}$  and  $U=4.4$  and  $8.8 \text{ eV}$ . The lines drawn are determined by least-squares fit to the data at normal incidence and correspond to a power of  $2.8 \pm 0.2$ .

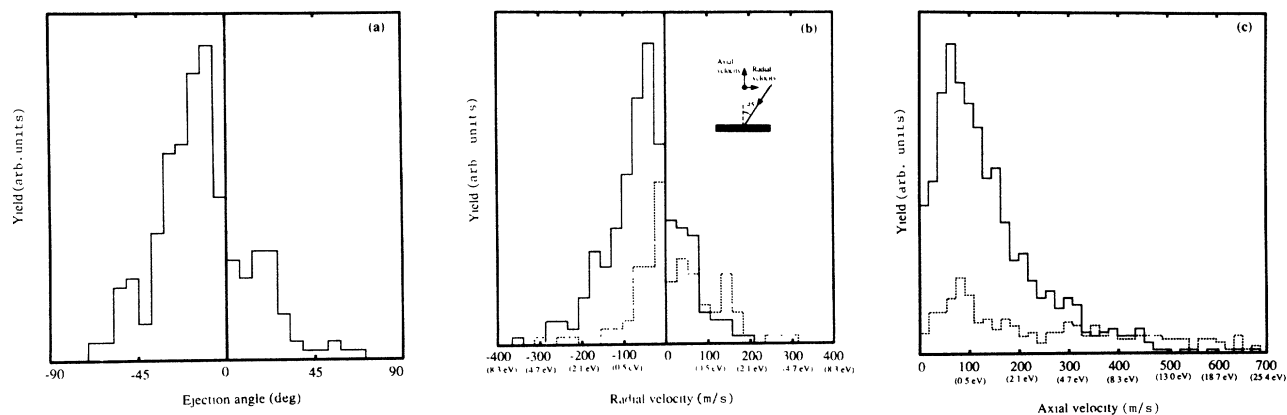


FIG. 6. Histogram of the intensity of nonexpanded molecules (solid lines) and expanded molecules (dashed lines) vs (a) ejection angle, (b) radial velocity, and (c) axial velocity for  $45^\circ$  angle of incidence.

figures. The plotted distributions are the components, in the plane of incidence, of the ejection angle and the radial velocity for molecules with velocity vectors less than  $20^\circ$  out of the plane of incidence to be comparable with experiments. The results presented here for the ejection angles are nearly independent of the excitation density in the region where the yield varies as the cube of the excitation density.

For normal incidence the nonexpanded molecules are ejected in a symmetric ring around the point of impact with minimum intensity for normal ejection. As the angle of incidence is increased the ring becomes asymmetric. For  $45^\circ$  angle of incidence the distribution of the component, in the plane of incidence, of the ejection angle of the *nonexpanded* molecules is found to peak at  $\sim -20^\circ$  and for normal incidence at  $\sim 40^\circ$  [Figs. 6(a) and 7(a), respectively]. These results are qualitatively consistent with recent experimental observations for molecular ions of bovine insulin desorbed by heavy-ion bombardment.<sup>22</sup> That experiment gave larger ejection angles

( $\sim -50^\circ$  and  $\sim +45^\circ$  for  $45^\circ$  and  $0^\circ$  angle of incidence, respectively) but since the experimental results are for ions, measurements on angular distributions of neutral molecules are needed for a direct comparison. For normal incidence, our analytical approximation<sup>10</sup> and the shock wave model<sup>13</sup> gives an ejection angle of  $\pm 45^\circ$  for surface species ejected and an ejection angle of  $\sim -23^\circ$  for  $45^\circ$  angle of incidence which is remarkably consistent with the calculations presented here and also independent of  $(dE/dx)$ .

The radial velocity distributions [Figs. 6(b) and 7(b)] show the same characteristics as the angular distributions. The axial velocity distributions [Figs. 6(c) and 7(c)] show only a weak dependence on the angle of incidence. For  $45^\circ$ , the distribution peaks at slightly higher energy. The velocity distributions of *expanded molecules* [Figs. 6(b) and 6(c) and Figs. 7(b) and 7(c)] are similar to those of nonexpanded molecules except for the radial velocity distribution in Fig. 6(b). This distribution has a long tail at positive velocities.

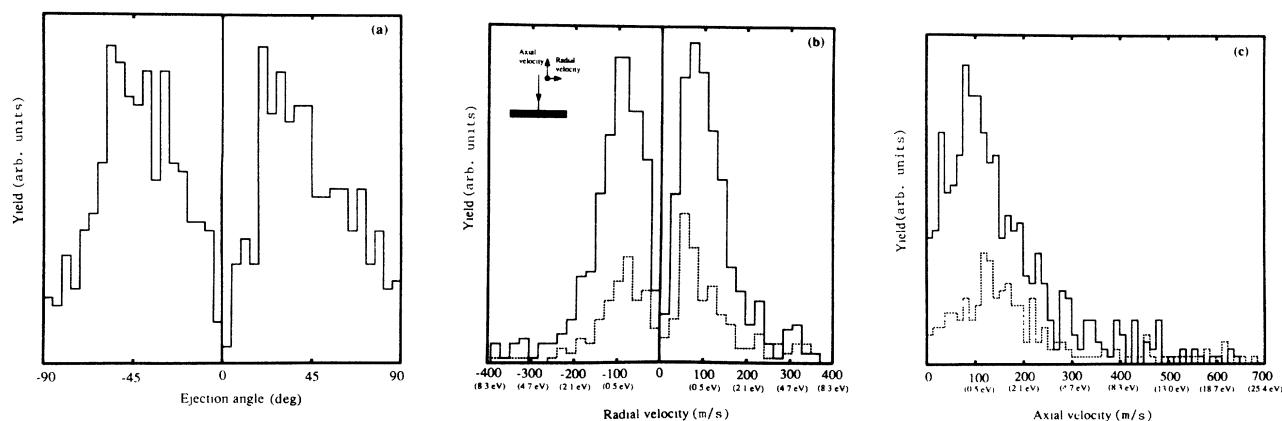


FIG. 7. Histogram of the intensity of nonexpanded molecules (solid lines) and expanded molecules (dashed lines) vs (a) ejection angle, (b) radial velocity, and (c) axial velocity for  $0^\circ$  angle of incidence.

## DISCUSSION

## Sputtering yield

To relate the expansion energy to the electronic stopping power of the incoming ion, the experimental results on total erosion yields of leucine<sup>19</sup> were used. A constant expansion of 12% inside a cylinder with a radius of 19 Å gives approximately the same total erosion yield as 90-MeV <sup>127</sup>I<sup>14+</sup>. This gives an expansion energy per unit path length which is ~1% of the electronic stopping power. That is, the expansion energy giving rise to the pressure contains only a small fraction of the energy deposited into the solid by the incident ion. The thermal energy required for 12% radial expansion was estimated to be ~1% of the electronic stopping power by using the thermal expansion coefficient. This shows that a high level of electronic excitation must result in only a modest amount of expansion energy in a short time in order to explain the measurements. Since this is an impulsive ejection process the amount of "expansion" energy required and the rate at which it occurs are closely related.

In our analytical approximation<sup>10</sup> it is assumed that the impulse propagation in the solid can be described either by a short pulse or by the diffusion equation. In either case the energy density in the solid is calculated as a superposition of contributions from each point along the ion trajectory. At high-energy densities, as in the simulations presented here, the energy gradient is large and a pressure pulse is created in the solid, in which case a simple criterion is used for ejection: molecules receiving an impulse larger than a critical impulse determined by the material cohesive energy are ejected. Using this criterion the total sputtering yield ( $Y_{\text{tot}}$ ) for normal incidence on an infinitely thick sample is

$$Y_{\text{tot}} = \frac{2\pi}{3} n_M \left[ \frac{\beta}{4\pi\kappa n_M p_c} \left( \frac{dE}{dx} \right)_{\text{eff}} \right]^3, \quad (6)$$

where  $n_M$  is the molecular density,  $\kappa$  an effective diffusivity,  $(dE/dx)_{\text{eff}}$  the effective stopping power,  $p_c$  the critical impulse for ejection, and  $\beta$  is  $(C_p/C_v - 1)$  for a gas. The critical impulse and the diffusivity can roughly be approximated by  $p_c = c_1(2UM)^{1/2}$  and  $\kappa = c_2(2U/M)^{1/2}n_M^{-1/3}$ , where  $c_1$  and  $c_2$  are constants,  $U$  is the material cohesive energy, and  $M$  the molecular mass. The yield, with these approximations, is written

$$Y_{\text{tot}} = \frac{(\beta c_1 c_2)^3}{(3)2^8 \pi^2 n_M} \left[ \frac{1}{U} \left( \frac{dE}{dx} \right)_{\text{eff}} \right]^3. \quad (7)$$

This gives roughly the same dependence on the energy deposition and the cohesive energy as do the simulations Figs. 5(a) and 5(b). A least-squares fit of Eq. (11) to the data for normal incidence in Fig. 5(a) gives  $\beta = 0.6 \pm 0.1$  when  $c_1 c_2 = 1$ . This is close to the value for a gas of structureless particles ( $\beta = 0.67$ ). Because the ejection in the simulations is dominated by interactions in the repulsive region of the potential, the system is fairly well approximated by a gas of particles,<sup>32</sup> so that the simulations and the analytical approximation give consistent sputtering yields. The sputtering can also be calculated numerically from the analytical approximation for a finite sample thickness. For this case the yield shows a transition from a cubic dependence on  $(dE/dx)_{\text{eff}}$  to an approximately linear dependence. The same trend is seen in the simulations for 45° angle of incidence [Fig. 5(b)]. However, the simple criterion used for ejection in the analytical approximation has limited applicability, hence, the need for molecular dynamics simulations in a number of instances.

## Angular and velocity distributions

When studying the angular and radial velocity distributions, it was found that the ejected molecules can be divided into different groups. One group consists of slowly moving molecules which have collided several times be-

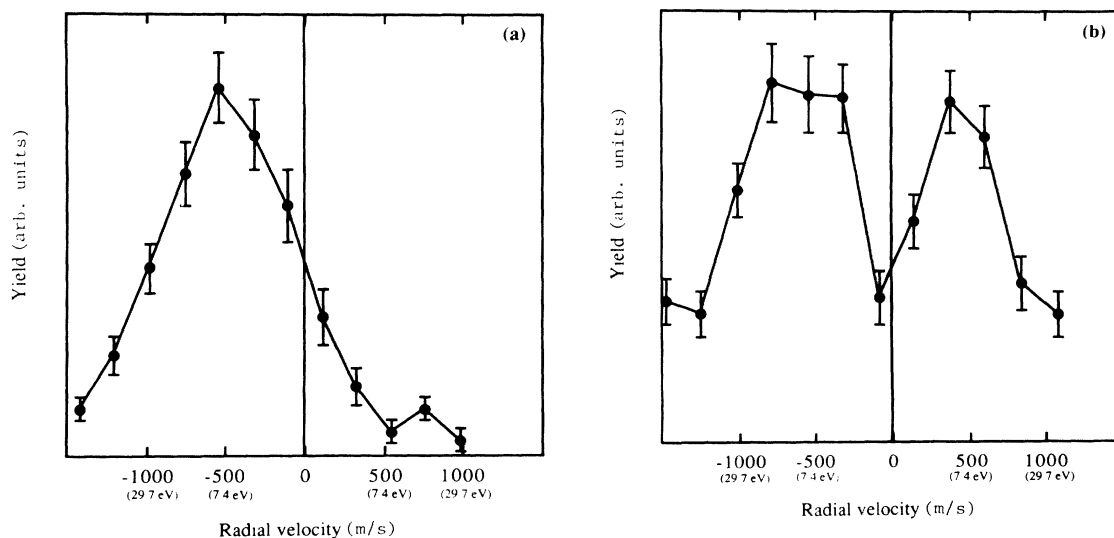


FIG. 8. Experimental results on radial velocity distributions of bovine insulin taken from Ref. 22. Angle of incidence of (a) 45° and (b) 0°. The results in (a) should be compared to the calculations in Fig. 6(b) and that in (b) to Fig. 7(b).

fore leaving the sample, or have been ejected in the form of clusters which eventually decay. The majority of the *nonexpanded* molecules will, however, be pushed out of the sample by a pressure emitted from the expanding track and subsequently propagate roughly perpendicular to the incident ion direction. This leads to characteristic angular distributions which depend on the angle of incidence.

The axial and radial velocity distributions for the nonexpanded molecules have centroids at lower velocities than that measured for whole molecular ions of insulin (Ref. 22 and Fig. 8). Due to the lower neutralization probability for faster molecules the ions ejected ( $\sim 10^{-3}$ – $10^{-4}$  of the total) involve only the energetic tail of the distributions calculated here. For this reason neutral velocity distributions tend to peak at lower velocities in most sputtering experiments. The smaller ejection angles calculated here, i.e., the fact that molecules are ejected in a direction closer to the normal of the surface than in the experiments for ion ejection, can partly be explained by differences of the sample surface. In the simulations, although the sample is amorphous, the surface is flat [Fig. 3(a)] while in the experiments surfaces with such flatness are impossible to produce. Due to the plane surface of the sample molecules are deflected and the angular distributions are shifted towards normal ejection. In future simulations samples with very rough surfaces can be used to evaluate this effect.

#### CONCLUSIONS

The calculations presented here show that a model in which the energy deposited by an ion is converted into

expansion of individual molecules leads to an impulsive ejection of material resulting in the formation of a crater in the sample. The molecular dynamics model used roughly explains the directional correlations between the incidence angle of the primary ion and the ejection angle of large molecules as well as the sputtering yield dependence on excitation density for the only experimental measurement available. It also confirms and quantifies the analytic model recently described. The remarkable simplicity in the nature of the "electronic" sputtering process as described here can be used to unify the large body of experimental data gathered since the discovery of this process and it also lends itself to an analytical approximation which can be used to understand certain basic aspects of the sputtering process. Although the model used here is conceptually simple, the use of molecular dynamics in the field of electronic sputtering is promising and is ideally suited for describing the details of the ejection process in response to a variety of excitations. Measurements on neutral molecules are now needed in order to make further comparisons between simulations and experiments.

#### ACKNOWLEDGMENTS

We acknowledge stimulating discussions with A. Hedin, P. Håkansson, and O. Tapia. The work was supported by the Swedish National Board for Technical Development and the Swedish Natural Research Council.

- 
- <sup>1</sup>D. F. Torgerson, R. P. Skowronski, and R. D. Macfarlane, *Biochem. Biophys. Res. Commun.* **60**, 616 (1974).
- <sup>2</sup>G. Jonsson, A. Hedin, P. Håkansson, B. U. R. Sundqvist, H. Bennich, and P. Roepstorff, *Mass. Spectrom.* **3**, 191 (1989).
- <sup>3</sup>See, for example, R. H. Stulen and M. L. Knotek, *Desorption Induced by Electronic Transitions (DIET III)* (Springer-Verlag, Berlin, 1989).
- <sup>4</sup>W. L. Brown and R. E. Johnson, *Nucl. Instrum. Methods B* **13**, 295 (1986); J. Schou, *ibid.* **27**, 188 (1987).
- <sup>5</sup>A. Hedin, P. Håkansson, B. Sundqvist, and R. E. Johnson, *Phys. Rev. B* **31**, 1780 (1985).
- <sup>6</sup>R. E. Johnson, *Int. J. Mass Spectrum Ion Phys.* **78**, 357 (1987).
- <sup>7</sup>P. K. Haff, *Appl. Phys. Lett.* **29**, 473 (1976).
- <sup>8</sup>R. E. Johnson and B. Sundqvist, *Int. J. Mass Spectrum Ion Phys.* **53**, 337 (1983).
- <sup>9</sup>P. Williams and B. U. R. Sundqvist, *Phys. Rev. Lett.* **58**, 1031 (1987).
- <sup>10</sup>R. E. Johnson, B. U. R. Sundqvist, A. Hedin, and D. Fenyő, *Phys. Rev. B* **40**, 49 (1989).
- <sup>11</sup>R. D. Macfarlane and D. F. Torgerson, *Phys. Rev. Lett.* **36**, 486 (1976).
- <sup>12</sup>H. Voit, E. Nieschler, B. Nees, R. Schmidt, C. H. Schoppmann, P. Beining, and J. Scheer, *J. Phys. C* **2**, 237 (1989).
- <sup>13</sup>I. S. Bitsensky and E. S. Parilis, *Nucl. Instrum. Methods B* **21**, 26 (1987); I. S. Bitsensky, A. M. Goldenberg, and E. S. Parilis, *J. Phys. C* **2**, 213 (1989) (unpublished).
- <sup>14</sup>D. Fenyő, B. U. R. Sundqvist, B. Karlsson, and R. E. Johnson, *Phys. C* **2**, 33 (1989); D. Fenyő, A. Hedin, P. Håkansson, R. E. Johnson, and B. U. R. Sundqvist (unpublished).
- <sup>15</sup>H. M. Urbassek and J. Michl, *Nucl. Instrum. Methods B* **22**, 480 (1987).
- <sup>16</sup>P. Håkansson and B. Sundqvist, *Radiat. Eff.* **61**, 179 (1982).
- <sup>17</sup>P. Håkansson, E. Jayasinge, A. Johansson, I. Kamensky, and B. Sundqvist, *Phys. Rev. Lett.* **47**, 1227 (1981).
- <sup>18</sup>P. Håkansson, I. Kamensky, and B. Sundqvist, *Surf. Sci.* **116**, 302 (1982).
- <sup>19</sup>M. Salehpour, P. Håkansson, B. Sundqvist, and S. Widdiyasekera, *Nucl. Instrum. Methods B* **13**, 278 (1986).
- <sup>20</sup>A. Hedin, P. Håkansson, M. Salehpour, and B. U. R. Sundqvist, *Phys. Rev. B* **35**, 7377 (1987).
- <sup>21</sup>S. Widdiyasekera, P. Håkansson, B. U. R. Sundqvist, *Nucl. Instrum. Methods B* **33**, 836 (1988).
- <sup>22</sup>W. Ens, B. U. R. Sundqvist, P. Håkansson, A. Hedin, and G. Jonsson, *Phys. Rev. B* **39**, 763 (1989); W. Ens, B. U. R. Sundqvist, P. Håkansson, D. Fenyő, A. Hedin, and G. Jonsson, *J. Phys. C* **2**, 9 (1989).
- <sup>23</sup>S. T. Cui and R. E. Johnson, *Int. J. Quantum Chem.* (to be published).
- <sup>24</sup>B. J. Alder and T. E. Wainwright, *J. Chem. Phys.* **27**, 2147 (1957).



- <sup>25</sup>L. Verlet, *Phys. Rev.* **159**, 98 (1967).
- <sup>26</sup>J. Åqvist, W. F. van Gunsteren, M. Leijonmarck, and O. Tapia, *J. Mol. Biol.* **183**, 461 (1985).
- <sup>27</sup>J. B. Gibson, A. N. Goland, M. Milgram, and G. H. Vineyard, *Phys. Rev.* **120**, 1229 (1960).
- <sup>28</sup>H. H. Andersen, *Nucl. Instrum. Methods B* **17**, 321 (1987).
- <sup>29</sup>B. J. Garrison and R. Srinivasan, *J. Appl. Phys.* **57**, 2909 (1985).
- <sup>30</sup>S. L. Lee and R. R. Lucchese, *J. Phys. C* **2**, 231 (1984).
- <sup>31</sup>R. E. Johnson, *J. Phys. C* **2**, 251 (1989).
- <sup>32</sup>P. Sigmund and C. Claussen, *J. Appl. Phys.* **52**, 990 (1981).